Initial state fluctuations in collisions between light and heavy ions

Brian Baker, Jordan Singer, Kevin Welsh, and Ulrich Heinz*
Department of Physics, The Ohio State University, Columbus, Ohio 43210-1117, USA
(Dated: July 27, 2015)

blah blah ...

PACS numbers: 25.75.-q, 12.38.Mh, 25.75.Ld, 24.10.Nz

I. INTRODUCTION

[This should go near the intro] To examine the effects of fluctuations on the initial entropy density distribution, eccentricity is used as a measure of the deformity of a distribution. Of primary interest are the lower order eccentricities, ϵ_2 and ϵ_3, which are linearly proportional to the corresponding final state flow coefficients. These are defined by

$$\epsilon_n e^{in\phi_n} = -\frac{\int r dr d\phi r^n e^{in\phi} \frac{d^2S(r,\phi)}{dr d\phi}}{\int r dr d\phi r^2 \frac{d^2S(r,\phi)}{dr d\phi}} \tag{1}$$

$$\epsilon_n \propto v_n, \forall n \in \{2,3\} \tag{2}$$

II. MODELING THE INITIAL STATE OF COLLISIONS BETWEEN LIGHT AND HEAVY IONS

A. Quantum fluctuations on the nucleon level

1. Fluctuating nucleon positions

To generate the initial configuration of the colliding nuclei, the Monte-Carlo Glauber model was used. For large nuclei, such as Au or Pb, the positions of their constituent nucleons are sampled from a Woods-Saxon distribution, imposing a hard-core radius (minimum inter-nucleon distance of 0.9fm [1]). With this generation scheme, a projectile proton is placed at position $(x_p, y_p) = (\frac{b}{2}, 0)$ in the transverse plane, where nucleus A is centered at position $(x_A, y_A) = (-\frac{b}{2}, 0)$. To generate a deuteron, our model first samples the relative nucleon separation according to the probability density obtained from the Hulthen wave function

$$P(r) = 4\pi r^2 |\Phi|^2 \tag{3}$$

$$\Phi(r) = \sqrt{\frac{\alpha\beta(\alpha+\beta)}{2\pi(\alpha-\beta)^2}} \frac{e^{-\alpha r} - e^{-\beta r}}{r}, \tag{4}$$

where $\alpha = 0.228$ fm^{-1} and $\beta = 1.18$ fm^{-1} (cite). Once the separation between the proton and neutron is sampled, the deuteron is given a random rotation in 3-space. For the ^{3}He and t nuclei, we used a set of 14,000 samplings of the positions of the three nucleons in these nuclei based on 3-body wave functions obtained from Green function Monte Carlo calculations using the AV18 + UIX model interaction [1]. This set of 3-nucleon configurations was kindly provided by (...). After centering the 3-nucleon systems at $(x_t, y_t) = (\frac{b}{2}, 0)$, we orient the sampled ^{3}He nuclei randomly in 3-space.

Nucleons in this model are described with a Gaussian probability distribution with a width controlled by the inelastic nucleon-nucleon cross-section σ_{NN}^{inel}. Projecting this Gaussian nucleon density distribution onto the transverse plane gives the nuclear thickness function [5]

$$T_N(r) = \frac{1}{(2\pi B)^2} e^{-\frac{r^2}{2B}}, \tag{5}$$

where the Gaussian width parameter B depends on collision energy, $\sqrt{s}$, through the inelastic nucleon-nucleon cross sections

$$B(\sqrt{s}) = \frac{\sigma_{NN}^{inel}(\sqrt{s})}{14.30} \tag{6}$$

This implementation differs from the popular choice of modeling the nucleons as cylindrical disks with axes along the beam direction by allowing, with small probability, inelastic collisions between nuclei that are separated by more than two mean nucleon radii in the transverse plane. Due to the nonzero tail of the nucleon shape, the average distance between two colliding nucleons is larger with our Gaussian shape than with the disk-like shape. This has important consequences in the ellipticity of very peripheral p+Au and p+Pb collisions. For each projectile nucleon from nucleus A at transverse position $\vec{X}_{\perp i}$, we now compute its collision probability with any of the nucleons in the target B at position $\vec{X}_{\perp j}$ as

$$P_{ij} = (1 - e^{-\sigma_{gg} T_{NN}(|\vec{X}_{\perp i} - \vec{X}_{\perp j}|)})_{i\in A, j\in B} \tag{7}$$

and vice versa. σ_{gg} is the gluon-gluon cross section and $T_{NN}(b)$ is the nucleon-nucleon overlap function [2]

$$T_{NN}(b) = \int d^2 r_\perp T_N(\vec{r_\perp}) T_N(\vec{r}_\perp - \vec{b}) = \frac{e^{-\frac{b^2}{4B}}}{4\pi B} \tag{8}$$

The nucleons (i,j) are labeled as wounded with probability P_{ij}. This procedure is performed on all pairs of projectile and target nucleons. No distinction is made

*Correspond to heinz.9@osu.edu

between nucleons that suffered one or more inelastic collisions - all of them are labeled as wounded. For each wounded nucleon, i, we now assume that it deposits entropy density in the transverse plane with a Gaussian distribution

$$\sigma_{NN,i}(\vec{r}_\perp) = \frac{e^{-\frac{|\vec{r}_\perp - \vec{r}_{\perp,i}|^2}{2B}}}{2\pi B} \tag{9}$$

The total initial entropy density at a given point in the transverse plane is then given by

$$S_o(\vec{r}_\perp) = \sum_{i=1}^{N_w} \frac{e^{-\frac{|\vec{r}_\perp - \vec{r}_{\perp,i}|^2}{2B}}}{2\pi B} \tag{10}$$

where N_w is the total number of wounded nucleons in the collision.

2. *Nucleon-nucleon multiplicity fluctuations*

An entropy deposition model which assumes each nucleon deposits the same total entropy in the transverse plane fails to replicate the distribution of multiplicities observed in p+p collisions. To correct for this, the total entropy that each wounded nucleon deposits is allowed to vary by an overall factor γ. To best fit the observed distribution, γ is sampled from a Gamma distribution

$$P(\gamma) = \frac{\gamma^{k-1} e^{-\frac{x}{\theta}}}{\theta^k \Gamma(k)} \tag{11}$$

with shape parameter k and scale parameter θ. This allows us to generate the new transverse entropy as

$$S_o(\vec{r}_\perp) = \sum_{i=1}^{N_w} \gamma_i \frac{e^{-\frac{|\vec{r}_\perp - \vec{r}_{\perp,i}|^2}{2B}}}{2\pi B} \tag{12}$$

This transverse entropy is then converted to the expected $\frac{dN_{ch}}{d\eta}$ from the collision by assuming they are linearly proportional

$$\frac{dN_{ch}}{d\eta} = \frac{K_s}{\tau_0} * \frac{4.8 * 0.75}{8.9} \frac{dS}{dy}\bigg|_{y=0} \tag{13}$$

Where K_s is a factor used to match the observed mean multiplicity. To allow for statistical variance, the actual resulting multiplicity is sampled from a Poisson distribution with mean $\mu = \frac{dN_ch}{d\eta}$. To generate figure 1, a sample of 500,000 p+Pb collisions at $\sqrt{s} = 5.02$ TeV were used. For each simulated event, the Poisson distribution was oversampled 5 times, resulting in 2.5 million data points. The choice for parameters K_s, and θ were taken from [5].

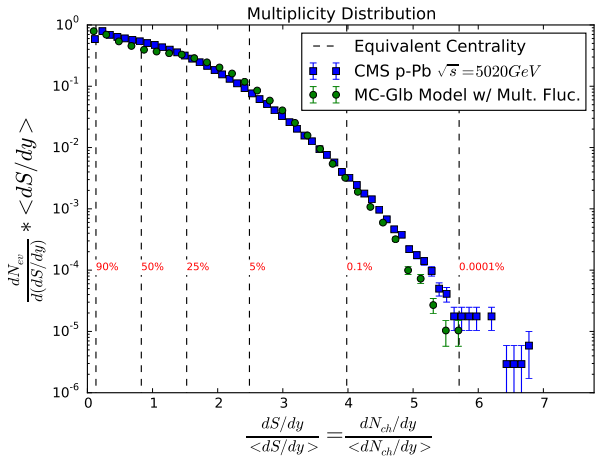

FIG. 1: Distribution of observed and simulated multiplicities assumed to be proportional to total entropy. Red numbers are estimates for centrality as determined from fraction of multiplicity. Fit parameters are $\theta = 0.75$,$k = \frac{1}{\theta} = 1.33$

B. Quantum fluctuations on sub-nucleonic length scales

In heavy ion collisions, event-by-event fluctuations in nucleon position play a crucial role in determining anisotropies in the transverse entropy density distribution. However, light ion collisions show a larger dependency on smaller scale fluctuations in nucleon multiplicity and sub-nucleonic entropy density, due to fluctuations in the gluon field and valence quark positions.

1. *Quark subdivision of nucleons*

We suggest that a more physical model of a nucleon considers the positions of each valence quarks, and treats them as Gaussian gluon sources. To account for this, the positions of these quarks were randomly sampled from a Gaussian distribution about the center of the nucleon with width $\sqrt{B}$. The gluon density around these quarks was then modeled by a separate Gaussian distribution about each quark position with width $\sigma_g = 0.2$fm. The effective width of the nucleon entropy deposition is

$$\sigma_{eff}^2 = \sigma_g^2 + B \tag{14}$$

With quarks now providing the base Gaussian entropy density distribution, the multiplicity fluctuation factor γ_q is sampled for and applied to the entropy density attributed to each quark.

$$\gamma_n = \sum_{i=1}^{3} \gamma_{qi} \tag{15}$$

FIG. 2

To maintain the same event-by-event multiplicity distribution, the PDF parameters must have the following relationships.

$$\theta_q = \theta_n \tag{16}$$

$$k_q = \frac{k_n}{3} \tag{17}$$

These considerations change the shape of the nuclear thickness function, $T_N(\vec{r})$, and the resultant transverse entropy deposition, $S_i(\vec{r} - \vec{r_i})$. The nuclear overlap function is no longer given by eq 7, but is now

$$T_N N(\vec{b}) = \sum_{i=1}^{3}\sum_{j=1}^{3} \int d^2 r_\perp \frac{1}{4\pi\sigma_g^2} e^{-\frac{(\vec{r}_{j\perp}+\vec{b}-\vec{r}_{i\perp})^2}{4\sigma_g^2}} \tag{18}$$

Due to eq 14, the average nuclear thickness over many events approaches a Gaussian with a width σ_{eff}. This means that the average collision probability is still given by $P(i,j)$. However, since $T_{NN}(\vec{b})$ is only non-zero when the valence quarks overlap, certain configurations are biased when deciding wounded nucleons, which affects the measured eccentricities. Figure 2 demonstrates this bias in p+p collisions at 200GeV.

2. *Sub-nucleonic gluon field fluctuations*

We introduce gluon field fluctuations in the entropy density of the wounded nucleons by first generating a 2D field of Gamma distributed random variables following the prescription of S. Moreland [3]. We define the resulting distribution to be $\Gamma(\vec{r}_\perp)$. To apply the fluctuations, a large (30 fm by 30 fm) field was generated from which to sample. For each nucleon i, a random square section is sampled from the grid with center $\vec{R}_i$ and width $10\sigma_p$. The entropy density distribution of each nucleon is modified by

$$S'_{0i}(\vec{r}_\perp) = S_{0i}(\vec{r}_\perp)\Gamma(\vec{R}_i + \vec{r}_\perp)\Theta(5\sigma_p - |\vec{R}_i - \vec{r_\perp}|) \tag{19}$$

When the nucleons are modeled by a single smooth Gaussian, these small scale fluctuations have a noticeable effect on the resulting eccentricities. However, when they are applied to a nucleon represented with quark substructure, they have a negligible effect when considering collision probability and resulting eccentricity. Also, we argue that it is unreasonable to account for gluon field fluctuations when ignoring the much larger scale effect of quark position. As such, future analysis will omit this effect in both the smooth Gaussian and fluctuating quark structure cases.

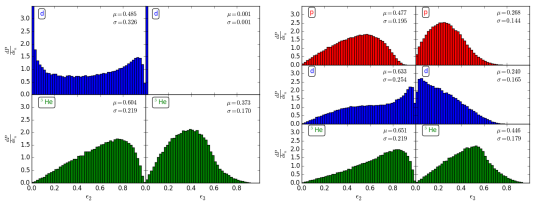

(a) **(b)**

FIG. 3: a shows the eccentricity distribution for the intrinsic structure of the deuteron, and ^{3}He. The smooth Gaussian proton is omitted, as its intrinsic entropy density is azimuthally symmetric. b shows the intrinsic eccentricity distributions when sub-nucleonic scale fluctuations are included. Since the quark sub-structure effectively replaces a proton with three smaller nucleons, one might expect that its profile would have a similar eccentricity to a ^{3}He nucleus. However, since there is no quark-quark exclusion, the quarks more easily overlap in the transverse plane than the repulsive nucleons of ^{3}He.

III. RESULTS

Unlike heavy ions, such as Au, light ions can exhibit intrinsic geometries that can bias certain eccentricities. For example, a deuteron only contains two nucleons, and as such, without sub-nucleonic fluctuations it is biased toward an elliptic deformation. Unfortunately, the influence that these intrinsic eccentricities have on the initial state anisotropies is not obvious. Figure 3 shows the distribution of these intrinsic eccentricities found in deuterons and ^{3}He nuclei with smooth Gaussian nucleons. Unintuitively, a ^{3}He nucleus has a significantly larger elliptic eccentricity than the deuteron, despite the elliptic symmetry in the deuteron being so apparent. This is because the eccentricities are calculated in the transverse plane. While a deuteron is more loosely bound than ^{3}He in 3-space, when projected onto the transverse plane it has a significantly smaller average intra-nuclear distance of 0.96 fm compared to 1.8 fm as determined from eq 3. Because a ^{3}He nucleus contains 3 nucleons that are not co-linear, it will always have some elliptic deformation in the transverse plane, which is on average larger than a deuteron's.

Naively, one would expect that these intrinsic geometries of light ions would appear in highly central collisions against a large nucleus, such as Au. However, figure 6 shows evidence that intrinsic eccentricity is a poor predictor of low centrality eccentricities. This is largely due to two unintuitive effects in the collision modeling system.

The first is the probabilistic binary collision detection method. Because the participation of two overlapping nucleons is determined by 7, the intrinsic geometry in the projectile nucleus is not guaranteed to carry over to the geometry of the wounded nucleons. Figure 4 reveals

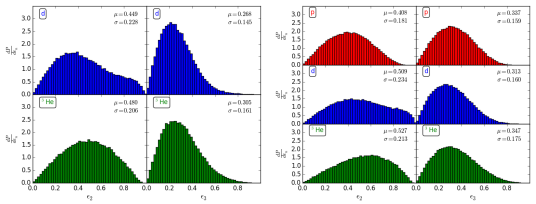

(a) Single Gaussian **(b)** Quark Sub-Structure

FIG. 4: a and b show the distribution of eccentricities in head on (b=0) x+Au collisions with single Gaussian and quark sub-structure nucleon representations.

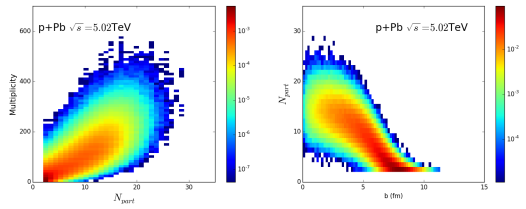

(a) **(b)**

FIG. 5

that collision geometries at b = 0 bear little resemblance of the intrinsic nucleon distributions, demonstrating that when colliding with a dense field of nucleons, the intrinsic geometry is not imprinted on the collision.

Secondly, centrality is an unintuitive metric. The centrality for these collisions was calculated relative to the largest multiplicity found in that collision type [5].

$$Centrality = \frac{1 - \frac{dN_{ch}}{dy}}{Max(\frac{dN_{ch}}{dy})} \tag{20}$$

In heavy-ion collisions, it is reasonably correlated with impact parameter and N_W. However, in light-heavy collisions, this is not the case. Figure 5 shows that multiplicity, N_W and impact parameter are only loosely correlated in light-heavy collisions. These correlations improve slightly as the size of the nuclei go up, but they are still poor in ^{3}He+Au collisions.

We have generated 500,000 MC-Glauber initial conditions for each collision type, x+Au at $\sqrt{s} = 200GeV$ and x+Pb at $\sqrt{s} = 5.02TeV$ where x $\in$ p,d,^{3}He. For each collision type, the eccentricities are plotted against centrality and impact parameter. Figure 7 shows the event-averaged elliptic and triangular flows of x+Au collisions against impact parameter. It includes graphs data for both the smooth Gaussian case, and the fluctuated quark substructure case. Nucleons at this energy have a Gaussian width of 0.40 fm. Figure 8 is the same, but with data from x+Pb collisions, where nucleons have a Gaussian width of 0.52 fm. In both, there are similar

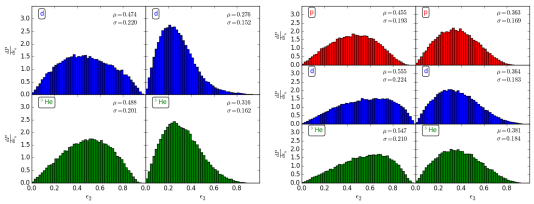

(a) **(b)**

FIG. 6: Distributions of ϵ_2 and ϵ_3 found in x+Au collisions with low centrality (0-10%). Neither with the smooth Gaussian model, a, nor with the added sub-nucleonic fluctuations, b, do the distributions resemble their intrinsic counterparts in FIG. 3.

trends. In the low impact parameter range, 0-4 fm, each curve is relatively flat. This is because the light nucleus is entirely contained within the heavy nucleus. The p+A curves peak at large impact parameters, as the average nucleon separation gets larger. The black curves for the p+p collisions act as a reference to demonstrate that the eccentricity is highly sensitive to the distance between wounded nucleons. In the smooth case, the triangularity comes only from the multiplicity fluctuations, which break the reflectional symmetry. Even this small, not inherently triangular effect can produce a large ϵ_3 when the wounded nucleons are spaced far enough away. This shows that while intrinsic geometry can bias certain eccentricities, other parameters, like average nucleon spacing, can be just as influential. Figures 9 and 10 com-

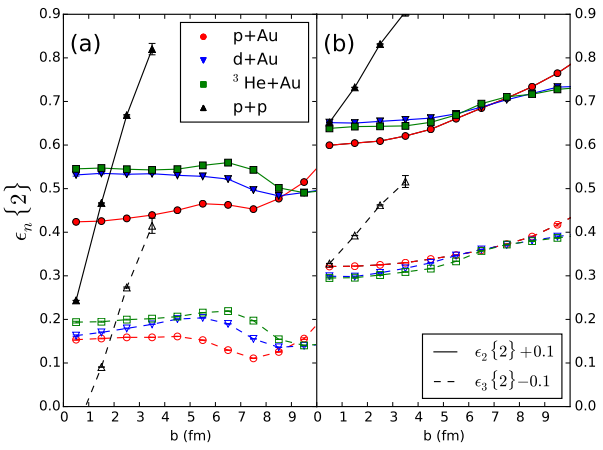

FIG. 7

prise our previous and updated expectations of experiments. They both show that the consideration of quark sub-structure has a large and complicated impact on initial state eccentricity. The most striking is that p, d and, ^{3}He + A collisions now produce very similar ϵ_3 curves. When considering ^{3}He+A collisions, one might expect that they would exhibit significantly higher ϵ_3 at most,

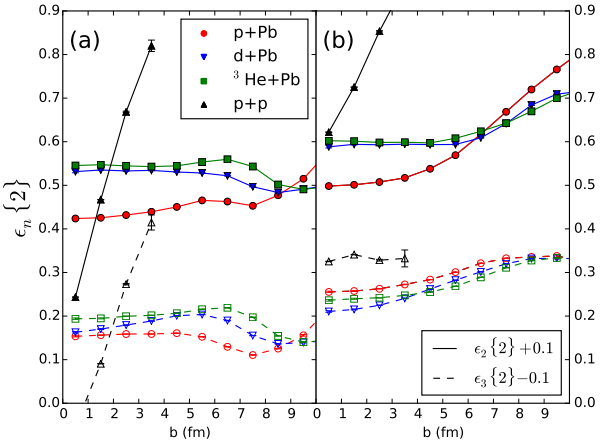

FIG. 8: Eccentricities Vs. Impact Parameter: Shown are MC Glauber initial conditions for both RHIC (top) and LHC (bottom) for the elliptical and triangular eccentricities in p+Au, d+Au, and ^{3}He+Au collisions as functions of impact parameter. In (a) the entropy density for the collisions is deposited as a smooth Gaussian distribution, while in fig (b) the entropy profile is texturized with sub-nucleonic scale fluctuations.

or all centralities. While this is the case with a smooth nucleon, the intrinsic geometry of ^{3}He is obscured when quarks are considered. Figure 10 even shows that ^{3}He has the smallest ϵ_3 from 30%-70%. This suggests that the random distribution of quarks washes out much of the intrinsic geometry found in light ions. As a result, the eccentricities are driven by collision parameters and, in part, measurement decisions.

Because centrality is measured relative to the max $\frac{dN_{ch}}{dy}$ of each collision type, different geometry biases appear. For example, low centrality d+A collisions are correlated with a low impact parameter, but are biased toward a larger deuteron; the average deuteron nucleon separation at 0-10% centrality is 15% larger than the minimum bias separation. This is because a larger deuteron will be able to hit more nucleons and generate a higher multiplicity. This is why we find a peak in the elliptic eccentricity at low centrality shown in figures 9 and 10, but do not in figures 7 and 8.

IV. SUMMARY AND CONCLUSIONS

Acknowledgments

We acknowledge fruitful and stimulating discussion with Jamie Nagle and thank Joe Carlson and Joel Lynn for providing us with 14,000 sampled nucleon configurations for ^{3}He nuclei using state-of-the-art 3-nucleon wave functions. This work was supported by the U.S. Department of Energy, Office of Science, Office of Nuclear Physics under Awards No. DE-SC0004286 and (within the framework of the JET Collaboration) DE-SC0004104. BB and KW gratefully acknowledge support through undergraduate summer research scholarships from the Department of Physics at The Ohio State University.

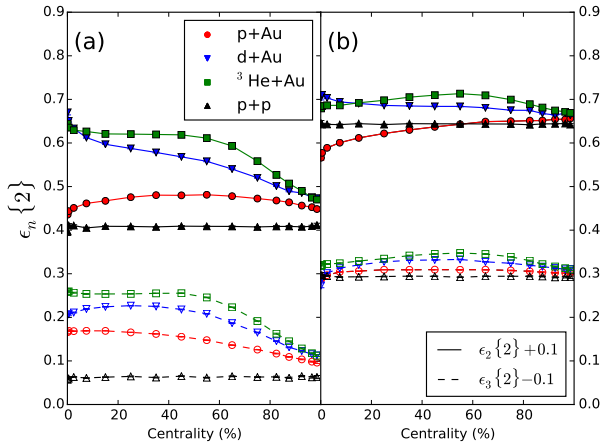

FIG. 9

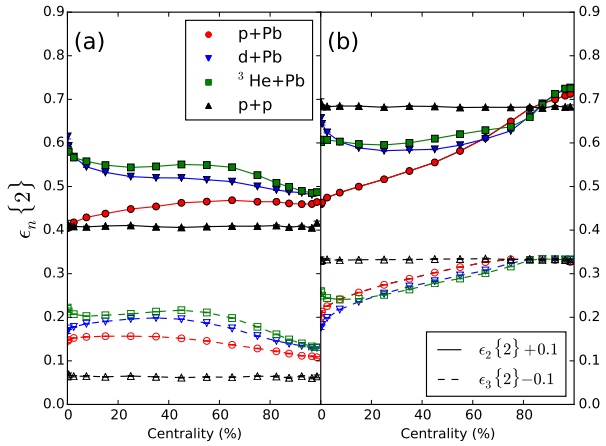

FIG. 10: Eccentricities Vs. Centrality: Centrality dependent eccentricities before (a) and after (b) the entropy density was texturized with sub-nucleonic fluctuations. Collisions were simulated for both RHIC (top) and LHC (bottom) energies

[1] J. Carlson and R. Schiavilla, Rev. Mod. Phys. **70**, 743 (1998).

[2] U. Heinz and J. S. Moreland, Phys. Rev. C **84**, 054905

(2011) [arXiv:1108.5379 [nucl-th]].
[3] J. S. Moreland, Z. Qiu and U. W. Heinz, Nucl. Phys. A **904-905**, 815c (2013) [arXiv:1210.5508 [nucl-th]].
[4] J. L. Nagle, A. Adare, S. Beckman, T. Koblesky, J. O. Koop, D. McGlinchey, P. Romatschke and J. Carlson *et al.*, Phys. Rev. Lett. **113**, no. 11, 112301 (2014) [arXiv:1312.4565 [nucl-th]].
[5] C. Shen, Z. Qiu, H. Song, J. Bernhard, S. Bass and U. Heinz, arXiv:1409.8164 [nucl-th].